SIEMENS

Experimental and Simulative Investigations of Conducted EMI Performance of IGBTs for 5 - 10 kVA Converters

Abstract

Power switches with high dv/dt and di/dt rates like IGBTs are the source of EMI. The paper presents investigations of conducted EMI on IGBTs in different test circuits. Moreover, results are explained from a special developed model for prediction of common and differential mode interferences, that is suitable to determine solutions for a better EMC through other design around the semiconductor chip. Results and further possibilities are discussed.

1 Introduction

IGBTs are mainly used in modern switched mode power supplies and power drive systems of middle power range. Ruggedness, blocking voltages up to 1600 V, high current densities and high switching frequencies are advantages of IGBTs. Requirements for high switching frequencies up to 20 kHz in hard switching converter applications, to reduce size and weight of passive energy stores and to increase the dynamic of the devices, are steep switching processes with dv/dt up to 15 kV/µs and di/dt up to 2 kA/µs for lower switch power losses. The electromagnetic interferences rise simultaneously. They can occur as radiated E- and H-fields and as conducted interference currents and voltages. This paper considers only conducted interferences.

2 Interference Mechanism

The conducted interferences are distinguished into asymmetrical and symmetrical interferences, common and differential mode respectively. **Figure 1** shows both phenomena.

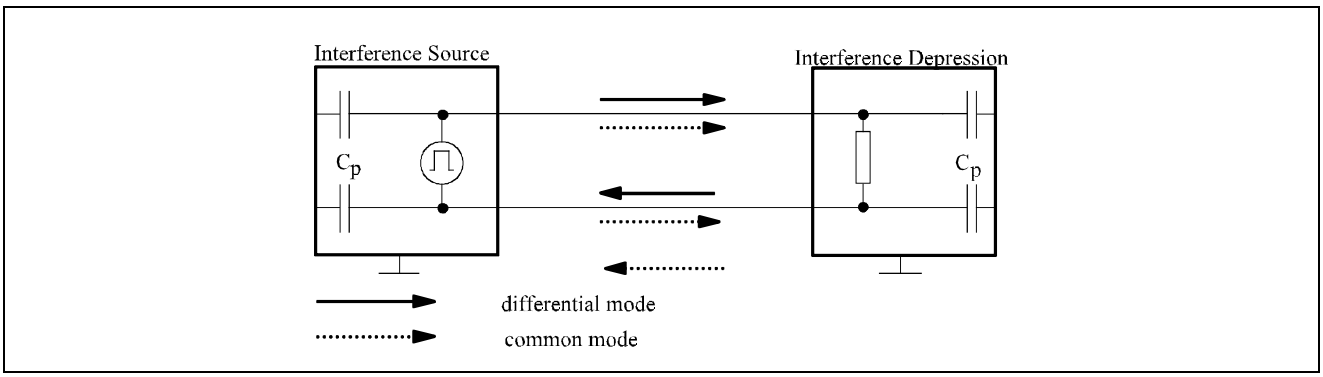

Figure 1
Conducted Interference Mechanism

The differential mode (dm) current only flows at the connecting line. The source of dm interferences is the current switched by IGBTs or diodes. High rates of dv/dt and parasitic capacitors to the ground are the reasons for common mode (cm) interferences. The cm circuit is closed across parasitic capacitors C_p to the earth ground and the connecting lines. The interference sink can be the main or another device connected with the source.

Periodical ideal rectangle functions in time domain generate a discrete line spectrum decreasing with 20 dB per decade in the frequency domain. The spectral lines are multiples of the basic frequency. Real wave-forms of switch cycles with turn on and turn off times t_a are rather trapezoid and have no constant repeat frequency. For that reason the spectrum decreases for $f < f_g$ { $f_g = 1/(t_a \pi)$} with 20 dB per decade and for $f > f_g$ with 40 dB per decade. The interference spectrum envelope is mainly used for the investigations of interference spectra.

The procedure of the signal analysis and transformation from the time domain in the frequency domain with Fourier-transformation and the interference spectrum envelope is represented in **Figure 2**.

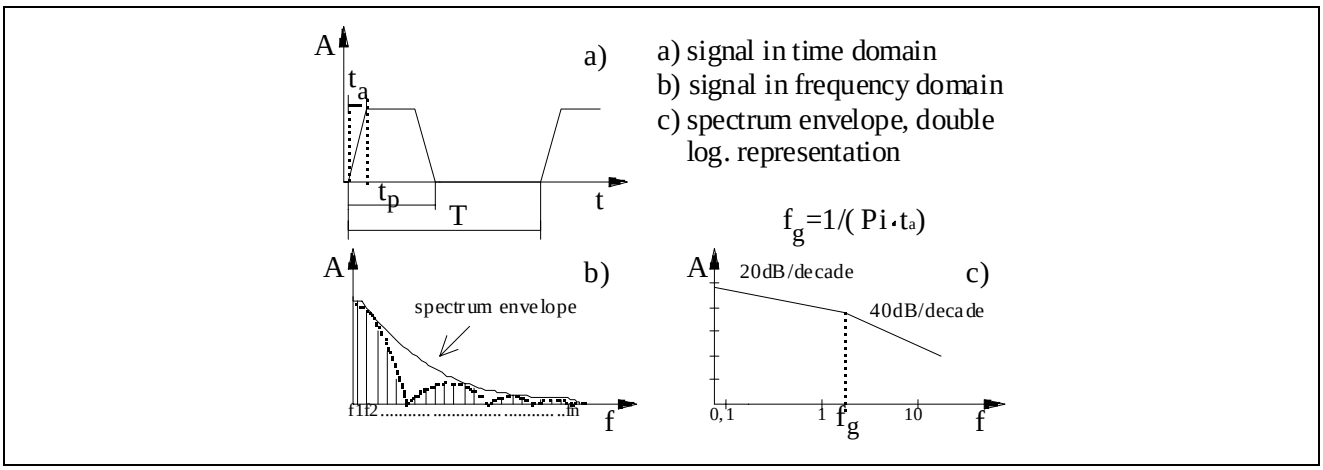

Figure 2
Analysis of Periodical Signals

3 Measurement

Test Circuit

A simple chopper, shown in **Figure 3**, was used as test circuit for the fundamental investigations of EMI performance of IGBTs.

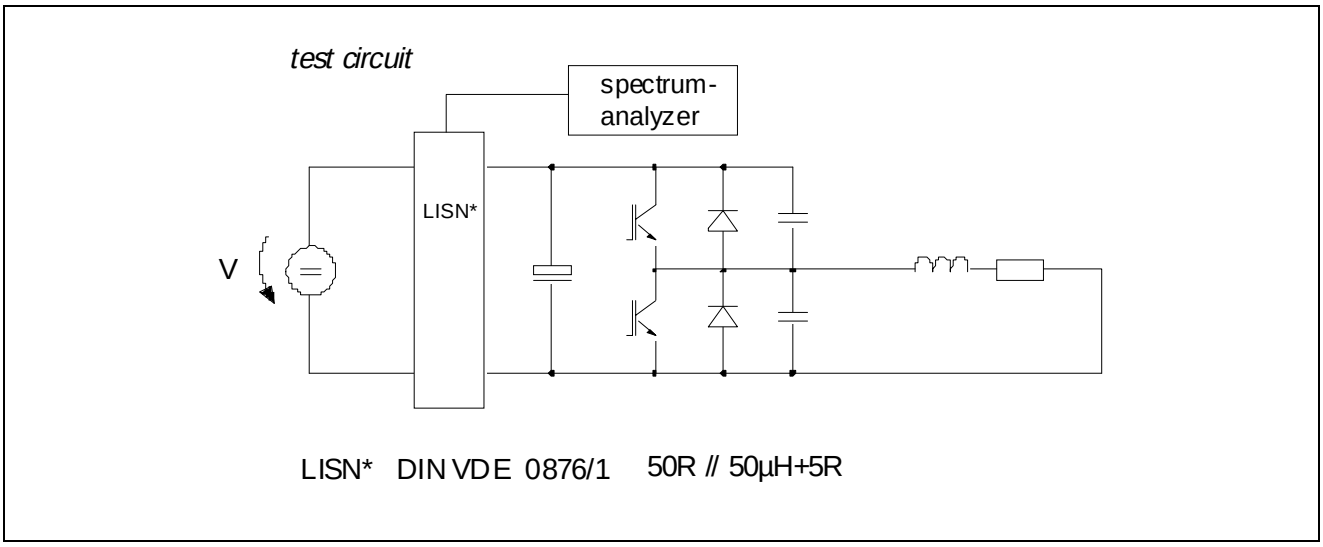

Figure 3
Chopper Test Circuit

The test circuit was connected directly to a Line Impedance Stabilisation Network (LISN 50 Ω // 50 µH + 5 Ω). This is necessary to obtain correct and reproductible measurement results and it is stipulated for measurements referring to international standards. The LISN is a low-pass filter between equipment under test (EUT) and main for both directions and prevents external noise coupling into the measurement. Moreover it is a high-pass filter to branch off the noise generated from the EUT to the spectrum-analyzer.

An adjustable DC-voltage source was used as power supply to avoid additional influences of interferences generated from a rectifier. A RL-combination with small parasitic elements was used as load.

Experimental Results

Several IGBT modules and single IGBTs and diodes in the 50 A/1200 V range were investigated referring to the EMI performance. Emphasis of investigations were the operating point (v, i, f_p), IGBT structure, module assembly (IGBT, diode, bonding, insulation), gate unit, temperature, earth ground conditions and additional elements. The measurement results were evaluated with the help of a developed model for prediction of common and differential mode interferences. Some examples of measurement results are shown in **Figures 4 - 8**.

Figure 4 shows spectra from several IGBT modules measured in the same operating point (OP) V_{CE} = 450 V, I_{CE} = 20 A, f_p = 5 kHz and switched with typical R_{Gon}/R_{Goff} from data sheets. All investigated IGBT structures (NPT and PT types) produce approximately the same interferences. The reason of differences in the spectra is the dependence of reverse

recovery behaviour of the free wheeling diodes on d*i*/d*t* rates. Therefore the faster switching NPT-types have some higher interference spectra in the frequency range above 3 MHz.

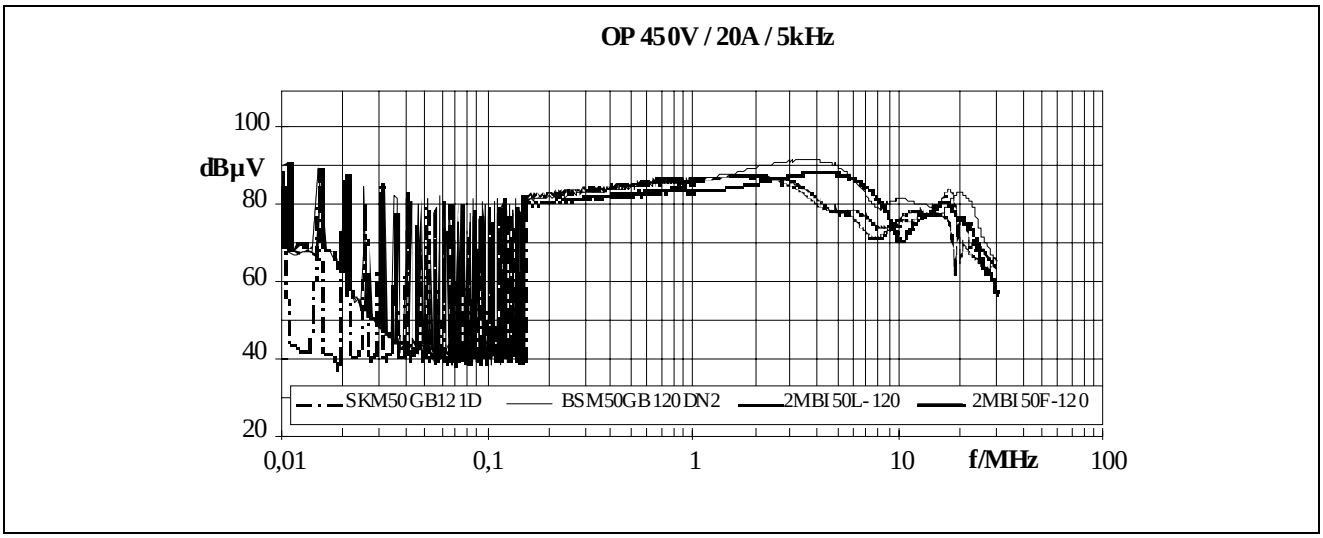

Figure 4
Spectra of Several IGBT Modules

Slower turn-on and turn-off transients reduce the d*i*/d*t* and d*v*/d*t* rates and change the reverse recovery current waveform of the diodes.

In the simplest way it is possible to investigate this aspect by changing the R_{Gon}/R_{Goff} resistances in the gate units. The results of this investigation are shown in **Figure 5**.

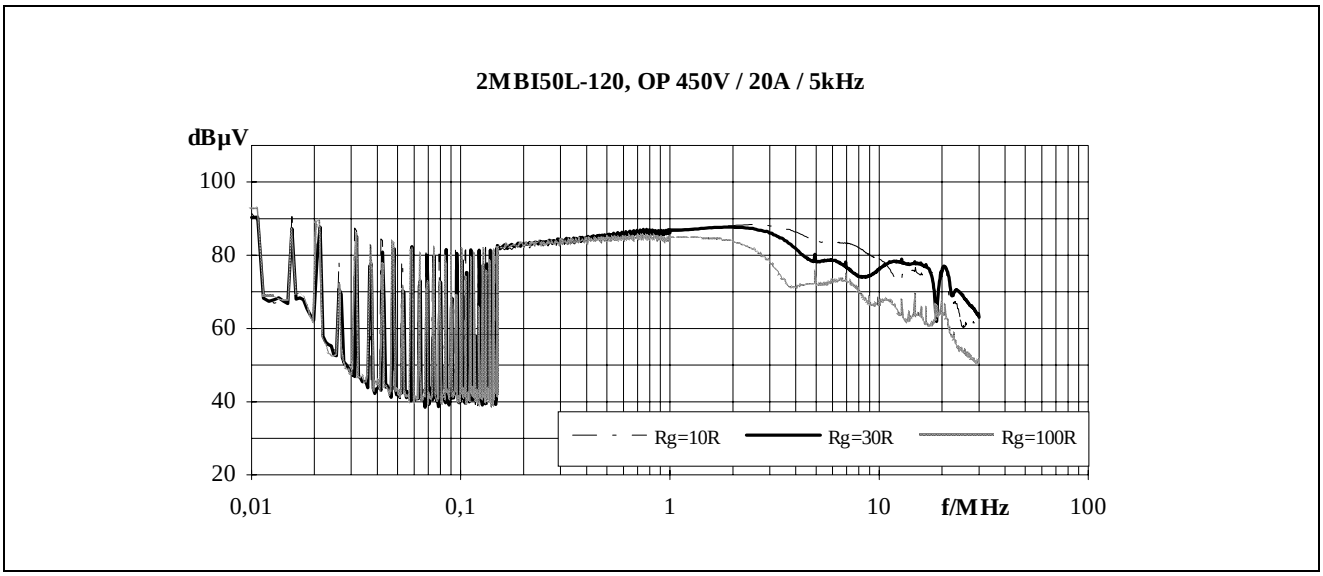

Figure 5
Interferences in Dependence on R_g

The interference spectra decrease with higher resistances but the switching losses rise during a cycle and restrict this approach. The interference spectra of the test circuit in this operating point are embossed by the load current from 10 kHz to 1 MHz and by the reverse recovery current of the free wheeling diode from about 1 MHz to 30 MHz. Both are dm

interferences. Above 200 kHz the spectra rise because the parasitic inductivity of the DC-link capacitors affects the impedance of the circuit for dm interference propagation.

The influence of additional capacitors connected directly at the module in parallel to the DC-link capacitors as a quasi short-circuit for high frequency dm interferences is shown in **Figure 6**.

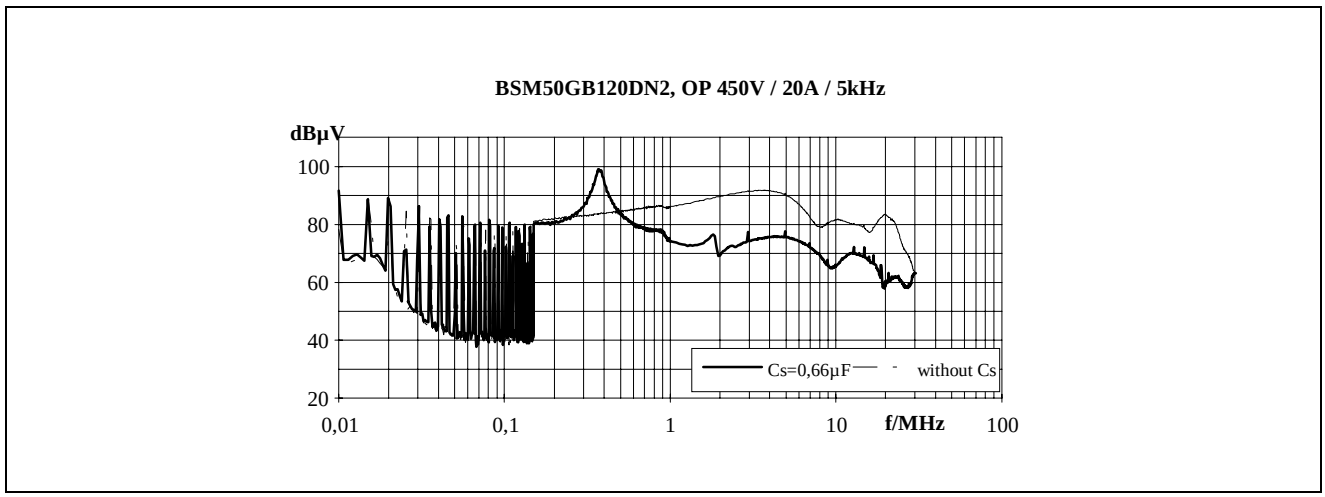

Figure 6
Capacitor C_s = 0,66 µF Across the Module

Behind the typical parallel resonance point caused by the additional capacitor C_s and parasitic inductivities up to the DC-link capacitor the interference spectrum decreases restricted by the own inductivity and resistance of C_s above 2 MHz.

A clear interference reduction by using RCD-circuits were not detected. The steepest flank affects mainly the interference form.

Figure 7 shows the problem of heatsink earthing in an other operating point (V_{CE} = 450 V, I_{CE} = 5 A, f_p = 5 kHz).

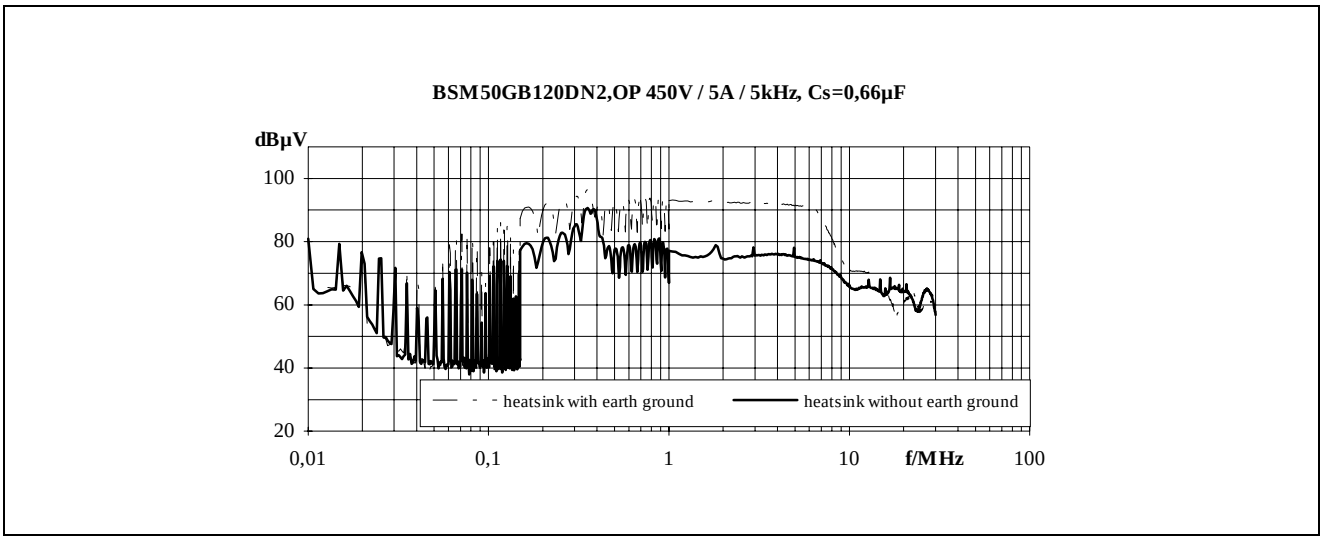

Figure 7
Earth Ground Conditions

The upper spectrum was measured at not grounded heatsink. If the heatsink is grounded the spectrum rises from 75 dBµV to about 92 dBµV above 200 kHz up to 8 MHz. This kind of interferences is detected as common mode interferences. High dv/dt rates initiate cm current through the parasitic capacities to the ground created by the insulation between IGBT collectors and diode cathodes to the heatsink. The value of parasitic capacitor C_p is dependent on area A, thickness d and dielectric constant ε of the insulation material (C_p = εA/d).

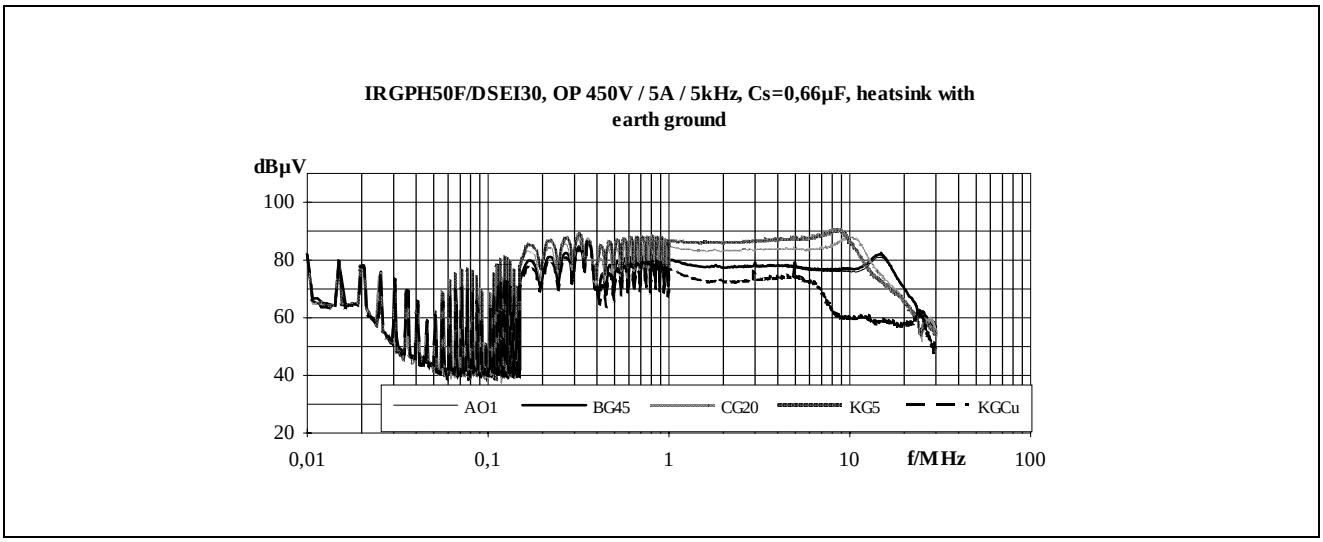

Figure 8
Influence of the Insulation Materials

Results of investigations of several insulation materials are shown in **Figure 8**. In dependence on insulation material the spectra vary in the frequency range above 500 kHz to 8 MHz between 72 dBµV and 88 dBµV. The highest level was measured by thin silicon rubber. Ceramic like Al_2O_3 proves to be better but the best result was reached with an in silicon rubber implemented copper screen connected to the DC voltage line.

The influence of temperature on the interferences is small and shall not be described. Only minor differences caused by the thermal dependence of reverse recovery behaviour were detected.

Operating point influences (v, i) are difficult to describe because of the complex relation between voltage and current (diodes behaviour). The common or the differential mode predominates in dependence on the circuit construction.

4 Investigations for Better EMC

Simulation

To get a better EMC it is necessary to analyse the main sources and spreading pathes of the interferences. The main problems of interferences in differential mode are the reverse recovery current of the free wheeling diodes and both parasitic inductivities of the capacitors and of the connecting lines between the capacitors. The parasitics reduce the interference depression and initiate resonance points shown in **Figure 6**. A reduction of interferences is possible by both decrease of the I_{RM} of the free wheeling diodes and reduction of the internal parasitic inductivities of the capacitors.

In the common mode the parasitic stray capacities C_p to the earth ground are problematic. **Figure 9** shows the geometrical assembly of IGBT modules.

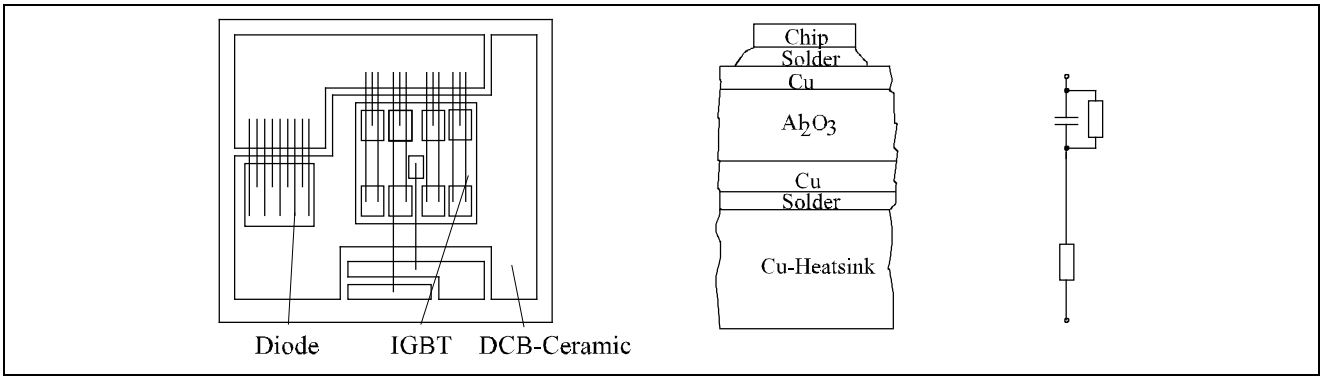

Figure 9
IGBT Module Assembly, C_p

The chip connected DCB area which has the high dv/dt-values causes the parasitic stray capacity with the insulation to the heatsink. For better cm interference depression the capacitor C_p must be minimized. This is limited possible by reducing the DCB surface arround the chip.

Several possibilities to reduce the interference propagation were tested by means of a simulation model for prediction of common and differential mode interferences based on

equivalent circuits of the physical power circuit layout including parasitics. The block diagram of the simulation model is shown in **Figure 10**.

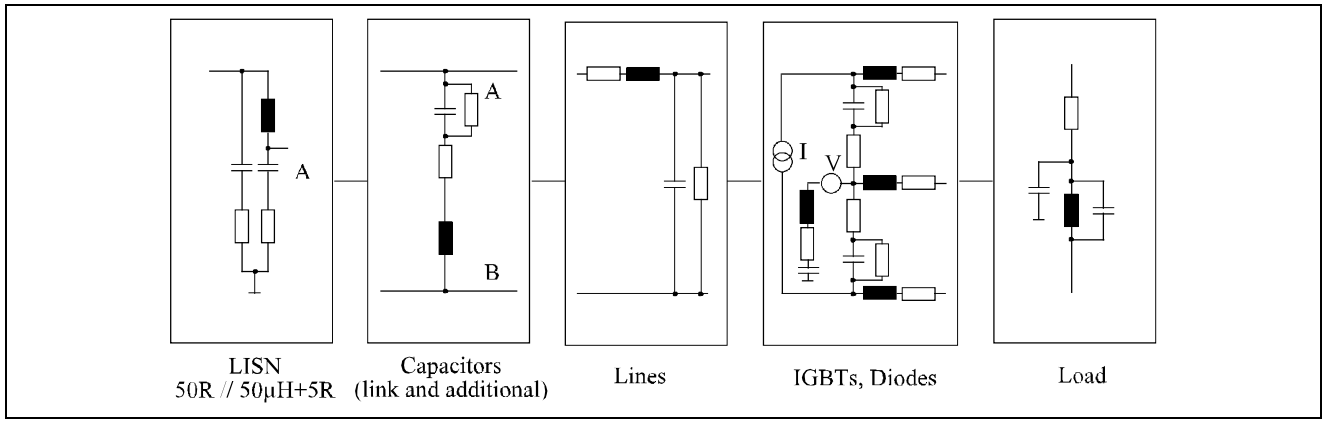

Figure 10
Simulation Model Block Diagram

The model makes it possible to distinguish the whole spectrum in common and differential mode components to determine seperatly a suitable design to avoid or reduce interferences.

Results of simulation are shown in **Figures 11 - 13**.

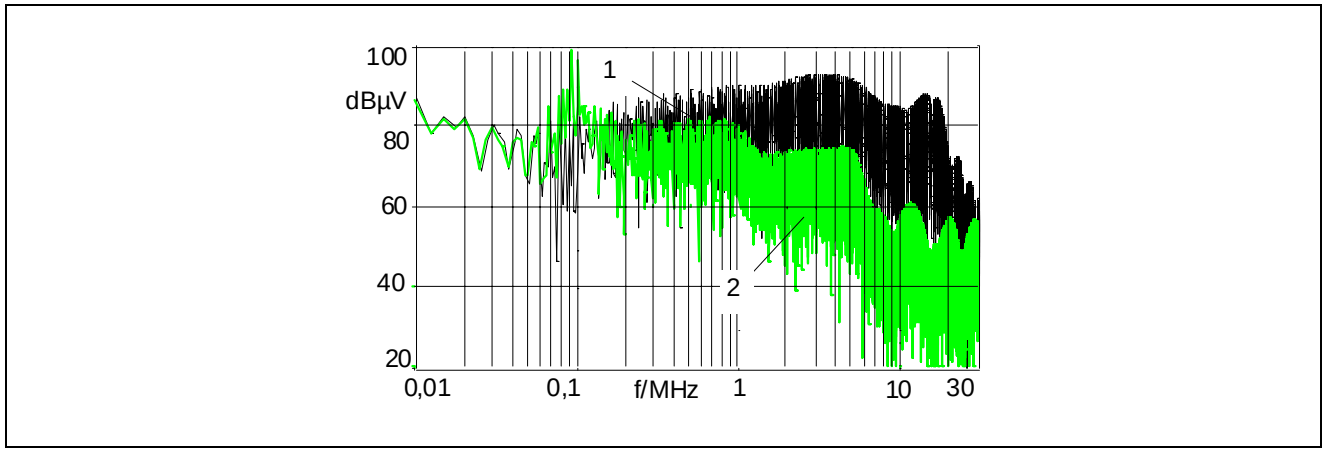

Figure 11
Predicted Interferences, Common and Differential Mode
1. Standard Module
2. Modified Module

Figure 11 presents the predicted whole spectra (cm, dm) of the standard module in comparison with a simulation of an improved module design. The calculating point is characterized by V_{CE} = 450 V, I_{CE} = 20 A, f_p = 5 kHz and a test circuit with grounded heatsink.

Some steps of interference reduction are separately presented in **Figure 12** (cm) and **Figure 13** (dm).The highest spectrum in **Figure 12** shows the standard module. The spectrum below it can be reached by elimination of the reverse recovery current I_{RM} of the free wheeling diodes by another diode design or by using soft switching principles.

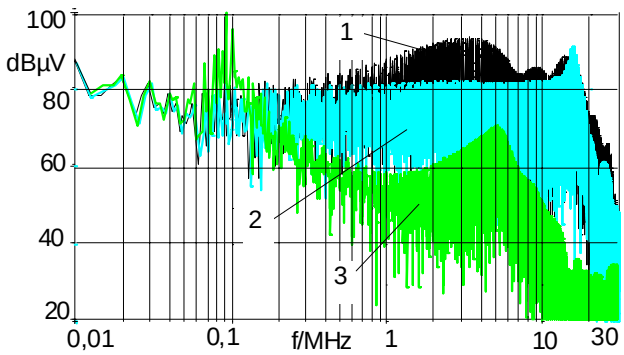

Figure 12
Influence of the Current on the Spectrum
1. Standard module
2. Standard module without I_{RM}
3. Modified module with C_{SC}

The lowest spectrum was calculated with an additional capacitor C_{SC} with minimal parasitic inductivities connected directly to the chip. The resonance point can be outside of the frequency range of the limit lines.

The highest spectrum in **Figure 13** was also calculated for the standard module. The spectrum below it can be reached by reduction of the parasitic stray capacities chip-heatsink from 130 pF to 60 pF through a reduced DCB surface in the approximate size of chip area.

The third and the fourth spectrum were calculated by using a low inductive conductive screen between chip and heatsink that is connected to the DC-line. In the third spectrum the interferences of the circuit are defined by parasitics of the load and the gate units. Spectrum number four in this figure and thus the best result was calculated without load parasitics. The interferences are less than 60 dBµV over the whole frequency range. The screen reduced the common mode interferences caused by the module by 30 dB. A disadvantage is a higher thermal resistance because of double insulation.

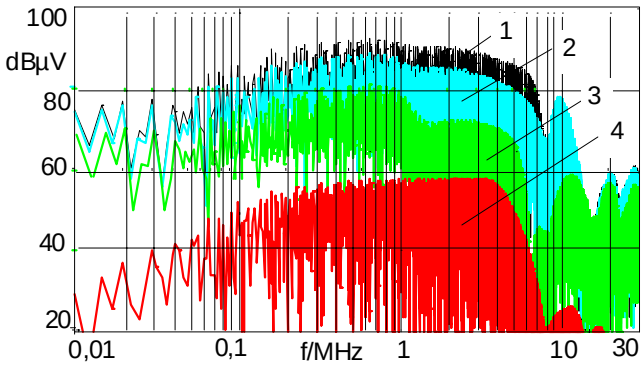

Figure 13
Interferences Initiated by the Switching Voltages
1. Standard module
2. Standard module with reduced DCB area
3. Modified module with load parasitics
4. Modified module without load parasitics

Measurement

The results of simulation were verified by experiments with modified IGBT modules. Additional capacitors were integrated inside of the module and a dc line connected screen was implemented.

A comparison between the measured spectra of standard and modified module is shown in **Figure 14**. The test circuit with modified modules generate a 15 - 25 dB lower EMI than standard modules.

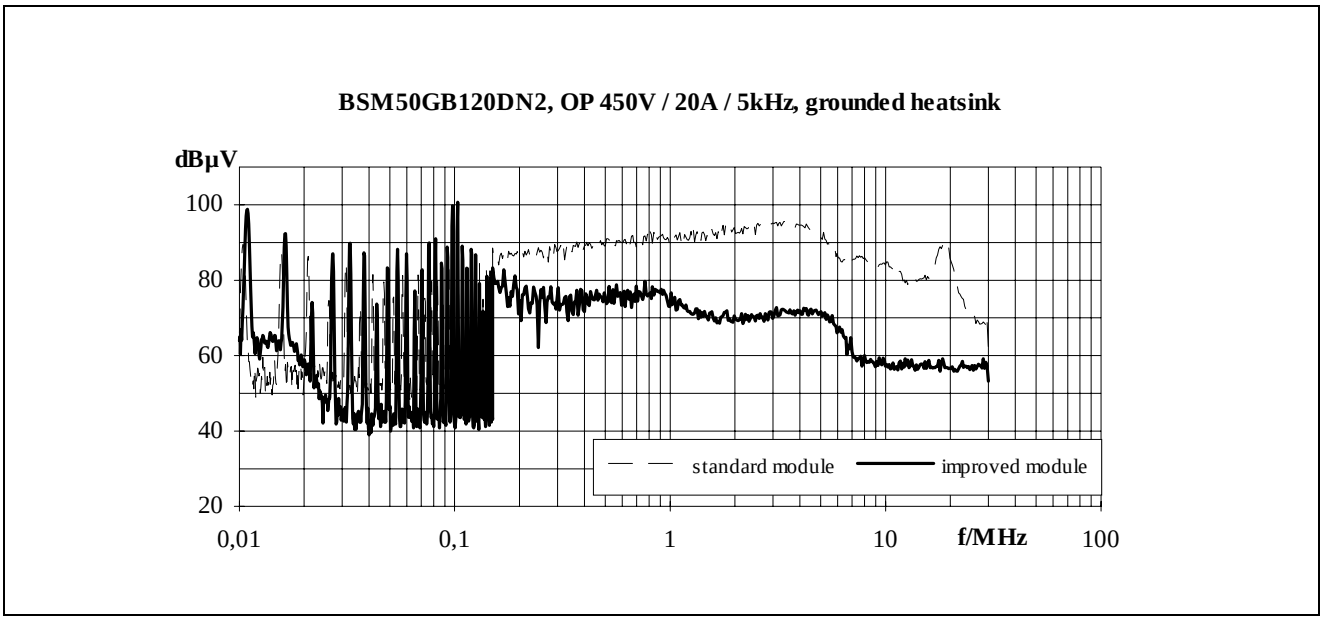

Figure 14
Spectra of Standard and Modified Module

Some examples of modified modules were tested under soft switching ZVS conditions in a full-bridge test circuit. Both the prevention of the I_{RM} of the diodes and lower dv/dt values effect a further reduction of the spectra. Results of variation of the dv/dt are shown in **Figure 15**.

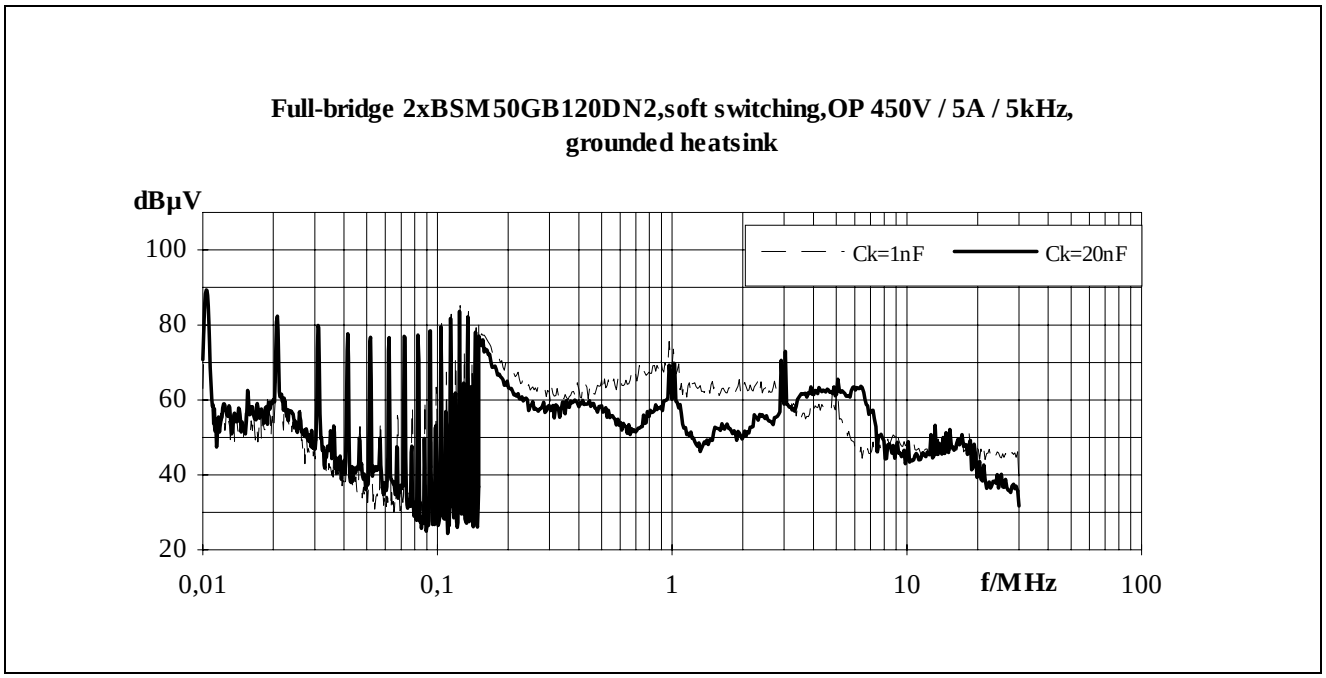

Figure 15
Modified Modules Under ZVS Conditions

By the reduction of the interference spectra generated by the power switches a further interference source is visible. The spikes at the spectra above 1 MHz result from the DC-DC-power supplies of the gate units that operate with a 1 MHz switching frequency. This interferences were not further considered.

5 Conclusion

The EMI performance of IGBTs was investigated under several conditions and influences. The investigations shown that the interference spectra are independent on the semiconductor structure. A mainly interference source in the differential mode is the reverse recovery current of the free wheeling diode. In the module assembly the spectra strong depend among other things on the chip to heatsink capacities. The used simulation model is suitable to analyse both interference modes and to determine better configurations with small expenditure. Experimental investigations at improved modules shown a reduced EMI. Load parasitics determine partly the interference spectra. By soft switching principles a rather interference reduction is possible.